Obscurin determines the architecture of the longitudinal sarcoplasmic reticulum

Stephan Lange[1,*], Kunfu Ouyang[1,*], Gretchen Meyer[2,3], Li Cui[1], Hongqiang Cheng[1], Richard L. Lieber[2,3] and Ju Chen[1,‡]

[1]Department of Medicine, University of California San Diego, 9500 Gilman Drive, La Jolla, CA 92093, USA
[2]Departments of Orthopedic Surgery and Bioengineering, University of California, La Jolla, CA 92093, USA
[3]VA Medical Center, San Diego, CA 92161, USA

*These authors contributed equally to this work
‡Author for correspondence (e-mail: juchen@ucsd.edu)

Accepted 17 April 2009
Journal of Cell Science 122, 2640-2650 Published by The Company of Biologists 2009
doi:10.1242/jcs.046193

Summary

The giant protein obscurin is thought to link the sarcomere with the sarcoplasmic reticulum (SR). The N-terminus of obscurin interacts with the M-band proteins titin and myomesin, whereas the C-terminus mediates interactions with ankyrin proteins. Here, we investigate the importance of obscurin for SR architecture and organization. Lack of obscurin in cross-striated muscles leads to changes in longitudinal SR architecture and disruption of small ankyrin-1.5 (sAnk1.5) expression and localization. Changes in SR architecture in obscurin knockout mice are also associated with alterations in several SR or SR-associated proteins, such as ankyrin-2 and β-spectrin. Finally, obscurin knockout mice display centralized nuclei in skeletal muscles as a sign of mild myopathy, but have normal sarcomeric structure and preserved muscle function.

Supplementary material available online at
http://jcs.biologists.org/cgi/content/full/122/15/2640/DC1

Key words: Ankyrin, Knockout, Muscular dystrophy, Nedd8, Obscurin, Sarcoplasmic reticulum

Introduction

It has long been known that the myofibrils of striated muscle cells are linked via an intricate filamentous network to the cell membranes (Clark et al., 2002; Pierobon-Bormioli et al., 1981). Recently, it emerged that complex cytoskeletal networks also support connections between myofibrils, and between the sarcomere and various organelles of the cell, including nuclei, mitochondria and the sarcoplasmic reticulum (SR). The entirety of these connecting filament systems (also known as extra-sarcomeric cytoskeleton) is thought to stabilize the sarcomeres in the context of the cytoskeleton, the myofibril-matrix and other organelles within the cell (Carlsson et al., 2008). Although the nature and composition of some of these filaments remained enigmatic for a long time, it has been suggested that giant proteins such as the nesprin (Zhang et al., 2001) and obscurin protein families (Bagnato et al., 2003) might play a role.

Obscurin (Obsc) was first described as a binding partner for Z-disc domains Z9 and Z10 of titin, but later was shown to have a more diverse localization within the sarcomere (Bang et al., 2001; Bowman et al., 2007; Carlsson et al., 2008; Young et al., 2001). Obsc belongs, like titin, to the class of giant proteins with a domain layout that is largely comprised of immunoglobulin-like (Ig) and fibronectin type III (Fn) domains. Interactions of the N-terminal Obsc Ig-domains with the M-band proteins myomesin and titin domain M10 establish the sarcomeric anchor point of the protein (Fukuzawa et al., 2008). It has been shown that mutations in the titin domain M10 abrogate binding to Obsc or its close homolog obscurin-like 1 (Obsl1) and might ultimately result in a form of limb-girdle muscular dystrophy (LGMD2J) (Hackman et al., 2002; Udd et al., 2005; Van den Bergh et al., 2003).

In addition to its modular Ig- and Fn-domains, Obsc contains a calmodulin IQ-binding motif and a predicted GDP-GTP exchange factor domain comprising a src homology (SH3), a dbl homology (DH), and a pleckstrin homology (PH) domain triplet near its C-terminus (Bang et al., 2001; Young et al., 2001) (Fig. 1D). Three major splice isoforms of Obsc have been reported. Alternative splicing near the Obsc C-terminal end adds two putative kinase domains to Obsc isoform B. These kinase domains can also be expressed independently by alternative promoter usage, resulting in an Obsc kinase-only protein KIAA1639/Obsc-kin (Borisov et al., 2008). Isoform A of Obsc and the putative 'Mini A' isoform of Obsc (Fukuzawa et al., 2005) contain a non-modular C-terminus that has been shown to interact with muscle-specific isoforms of ankyrin-1 (small ankyrin-1.5, sAnk1.5) and ankyrin-2 (Ank2) (Bagnato et al., 2003; Cunha and Mohler, 2008; Kontrogianni-Konstantopoulos et al., 2006; Kontrogianni-Konstantopoulos et al., 2003; Porter et al., 2005). These interactions of Obsc-A with sAnk1.5 and Ank2 suggest that Obsc might link the sarcomere to the SR and might participate in the organization and architecture of the SR (Bagnato et al., 2003; Cunha and Mohler, 2008; Kontrogianni-Konstantopoulos et al., 2003).

The SR is a complex three-dimensional membrane system that functions in muscle cells to store calcium, and contributes to calcium release and uptake during muscle contraction and relaxation (Rossi et al., 2008). Two structurally and functionally distinct parts of the SR can be delineated: the junctional SR in close proximity to the T-tubule system, and the longitudinal SR that connects the neighboring junctional SR along the myofibrils (Rossi and Dirksen, 2006). Junctional SR and T-tubules form a functional and structural complex that is referred to as 'diad' in heart, and as 'triad' in skeletal muscle cells. Diads and triads provide the structural basis for the excitation-contraction coupling in cross-striated muscle cells. At the molecular level, the major ion channels embedded in the junctional SR membranes are the ryanodine receptors (RyRs) (Rossi and Dirksen, 2006). The longitudinal SR emerges from the

Journal of Cell Science

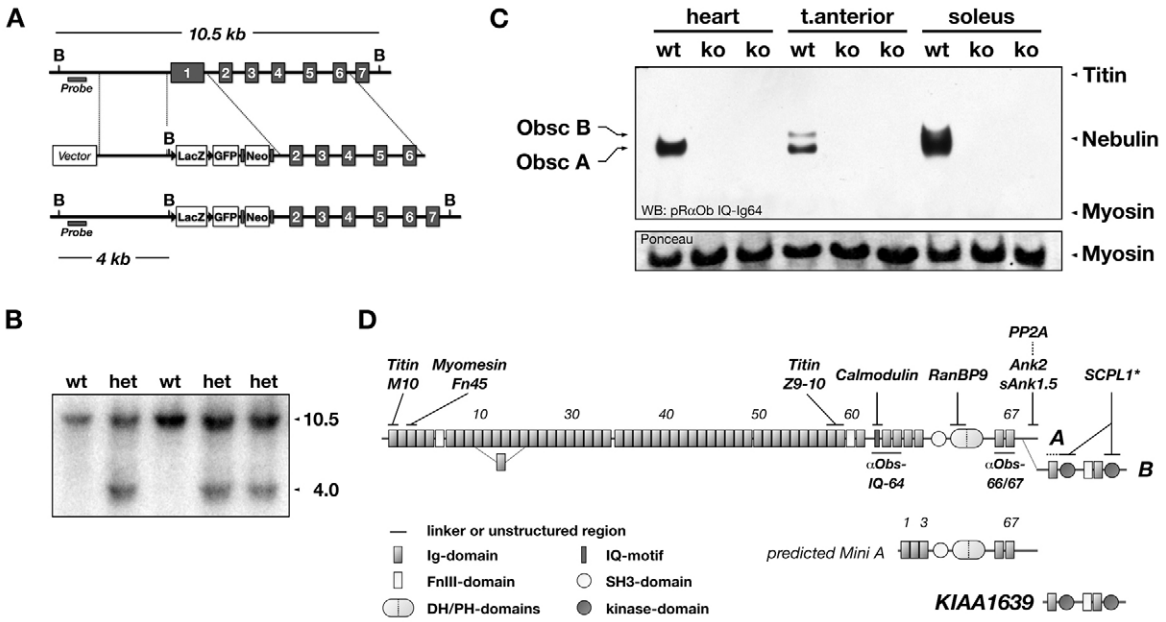

Fig. 1. Targeting of the obscurin gene and obscurin domain layout. (A) Cassette containing *lacZ*, *GFP*, and a *neomycin* gene under control of the *Mcl*-promoter, replaces coding exon 1 of murine obscurin, and effectively puts *lacZ* under control of the endogenous *Obscn* promoter. Black triangles mark *LoxP*-sites and grey rectangles *FRT*-sites. B denote BglII sites. The region used for the Southern-probe is marked. (B) Positively recombined embryonic stem-cell clones are identified by Southern blot analysis of their genomic DNA. The sizes (in kb) correspond to the expected theoretical values from A. Wild-type (wt) and heterozygous (het) clones are shown. (C) Total protein of heart, tibialis anterior and soleus muscles from *Obscn*$^{-/-}$ (ko) and wild-type (wt) littermates were separated on 1% SDS-agarose gels, immunoblotted and analyzed with an antibody raised against the IQ-Ig64 region of obscurin. No obscurin protein could be detected in any of the analyzed tissues derived from *Obscn*$^{-/-}$ mice. Bands in the wild-type tibialis anterior sample indicate two splice isoforms, obscurin A and B. Ponceau-red staining of myosin is shown as loading control. (D) Domain layout of Obsc-A and Obsc-B, the putative Obsc 'Mini-A', and the Obsc 'kinase-only' KIAA1639. Known interaction partners and their binding site are shown (asterisk indicates interactions demonstrated for unc-89). The obscurin antibody epitopes and domain types and numbers are denoted. Ig, immunoglobulin-like; FnIII, fibronectin type III; SH3, src homology 3; DH, double homology; PH, pleckstrin homology; Ank, ankyrin; SCPL1, serine carboxypeptidase-like 1; PP2A, protein phosphatase 2A.

junctional SR and continuously branches out to form an intricate network anastomosing along the myofibrils. At the level of the M-band the longitudinal SR occasionally forms a 'fenestrated collar' (Dalen et al., 1987). To date, very few proteins have been localized to the longitudinal SR membrane. Among them are several ankyrin isoforms, with sAnk1.5 being the best characterized (Rossi and Dirksen, 2006).

The ankyrin protein family is comprised of three members: ankyrin-1 (ankyrin-R), ankyrin-2 (ankyrin-B) and ankyrin-3 (ankyrin-G) (Bennett and Chen, 2001; Cunha and Mohler, 2006). A characteristic feature of all ankyrins is their domain layout: N-terminal ankyrin repeats, a central spectrin-binding domain, and a C-terminal death domain. The ankyrin repeats associate the ankyrin proteins to the membranes owing to their interaction with ion channels such as the sodium-calcium exchanger (NCX1) or RyRs (Mohler et al., 2005). The central spectrin-binding domain is important for the association of ankyrin to the spectrin filaments (Mohler et al., 2004). This interaction might be regulated by ubiquitin as ankyrin and α-spectrin are targets for the E2 and E3 activity of spectrin (Chang et al., 2004). The proposed role of ankyrin proteins lies in their ability to organize membrane architecture and coordinate protein trafficking to membranes (Cunha and Mohler, 2006). Mutations in ankyrin proteins have been linked to a number of human diseases, like the ankyrin-B syndrome (long QT syndrome 4) (for a review, see Mohler, 2006). Mice deficient in Ank2 have been shown to develop severe congenital myopathy that is associated with dramatic alterations in the intracellular localization of SR calcium homeostasis proteins (Tuvia et al., 1999).

The muscle-specific sAnk1.5 (Gallagher and Forget, 1998) is unique among the ankyrins by featuring none of these typical domain types. It features a distinctive N-terminal transmembrane domain (Porter et al., 2005), and two conserved cytoplasmic Obsc-binding domains (OBDs) (Borzok et al., 2007). OBDs have also been identified in a newly discovered splice isoform of Ank2 (Cunha and Mohler, 2008). Lastly, a sAnk1.5-specific knockout has been reported that shows weaker contractile performance and a lowered fatigue resistance (Quarta et al., 2007); however, SR protein localization was unaltered.

To investigate the importance of the Obsc-ankyrin interaction for SR organization and architecture, and to discern the significance of the sarcomeric interactions of Obsc with titin and myomesin at the M-band with respect to the development of LGMD2J in humans, we generated mice that lack the giant protein Obsc. We report that obscurin is important for longitudinal SR architecture and the maintenance of sAnk1.5 expression levels. Furthermore, we demonstrate that skeletal muscles of *Obscn*$^{-/-}$ mice show centralized nuclei in an age-dependent manner.

Results

Generation of the obscurin knockout

To investigate the biological role of Obsc in vivo, particularly its impact on sarcomeric structure and SR architecture, we generated mice deficient in Obsc. The targeting strategy inserted a *lacZ* reporter gene cassette under the control of the endogenous *Obscn* promoter, effectively replacing Obsc-exon 1 (Fig. 1A). To confirm the successful targeting of the *Obscn* gene, we analyzed genomic

Journal of Cell Science

DNA of targeted ES-cells by Southern blot (Fig. 1B). Disrupted Obsc expression was validated using semiquantitative RT-PCR on mRNA isolated from skeletal and heart muscle, as well as immunoblot analysis of heart and skeletal muscles from wild-type and *Obscn*$^{-/-}$ mice, respectively (Fig. 1C, supplementary material Fig. S1A,Ba-e). Whereas expression of obscurin (isoforms A and B) was not detectable at mRNA and protein level in all analyzed *Obscn*$^{-/-}$ tissues, expression of the kinase region of obscurin (KIAA1639) was still detectable at the mRNA level, albeit at somewhat lower levels (supplementary material Fig. S1A,Bf,g). This result confirms previous findings (Bowman et al., 2007; Fukuzawa et al., 2005) that the obscurin kinase region might be independently expressed as KIAA1639 (Fig. 1D). *Obscn*$^{-/-}$ mice are viable and reproductive, have no obvious physiological or pathological abnormalities and generally appear healthy. Basal heart-body weight ratios of *Obscn*$^{-/-}$ mice are comparable to wild-type controls (not shown).

Obscurin is expressed in cross-striated muscles

We used the *lacZ* reporter under control of the endogenous *Obscn* promoter to perform X-gal staining of several mouse tissues to detect the tissue-specific expression pattern of endogenous obscurin. We only found positive β-galactosidase activity in striated muscle tissues (Fig. 2A). Obsc has been found to localize to several subcellular compartments within cross-striated muscles cells, notably the Z-disc, A-I junction as well as the M-band of the sarcomere (Carlsson et al., 2008). Moreover, the subcellular localization of obscurin was attributed to different Obsc isoforms (Bowman et al., 2007). According to our western blot analysis (Fig. 1C) both Obsc isoforms are expressed in tibialis anterior muscles, whereas heart contains almost exclusively isoform A. We also performed immunofluorescence analysis of wild-type skeletal and cardiac tissues to determine the subcellular Obsc localization. As shown in Fig. 2B (see also supplementary material Fig. S4), Obsc localizes to the sarcomeric M-band in cross-striated muscle cells, confirming previous results with other antibodies (Young et al., 2001). This result indicates that both Obsc isoforms localize to the sarcomeric M-band.

Normal sarcomeric structure in *Obscn*$^{-/-}$ mice

Several reports using RNAi techniques in mammalian cells (Borisov et al., 2006; Kontrogianni-Konstantopoulos et al., 2006), zebrafish (Raeker et al., 2006) and *Caenorhabditis elegans* (Small et al., 2004) indicated that Obsc or its homolog Unc89 might be essential for sarcomere formation and lateral alignment of the myofibrils. We employed antibodies against sarcomeric α-actinin and the N-terminal region of titin in order to analyze Z-disc structure (Fig. 2C), as well as antibodies against myomesin and titin-M8 to visualize the sarcomeric M-band (Fig. 2D) in *Obscn*$^{-/-}$ mice. No apparent abnormalities in Z-disc or M-band architecture could be observed at the light microscopic level, indicating that sarcomerogenesis and lateral alignment of myofibrils were unchanged in *Obscn*$^{-/-}$ mice compared to wild-type littermates.

Recently, obscurin-like 1 (Obsl1), a close homolog of Obsc, was also found to interact with myomesin and titin (Fukuzawa et al., 2008). This redundancy in protein functions between Obsc and Obsl1 might compensate for the loss of Obsc during sarcomerogenesis and for sarcomeric structure. In order to determine the effects of the absence of Obsc on Obsl1 and the sarcomeric structure, we tested the subcellular localization of Obsl1 in skeletal and cardiac muscle cells using different Obsl1 antibodies. As demonstrated in Fig. 2E, Obsl1 localizes to the M-band in both wild-type and *Obscn*$^{-/-}$ mice, indicating a putative rescue effect of the sarcomeric structure by Obsl1. However, the Obsl1 expression level remained unchanged in *Obscn*$^{-/-}$ mice compared to wild-type littermates (not shown), indicating the absence of a compensatory effect on the expression levels of Obsl1.

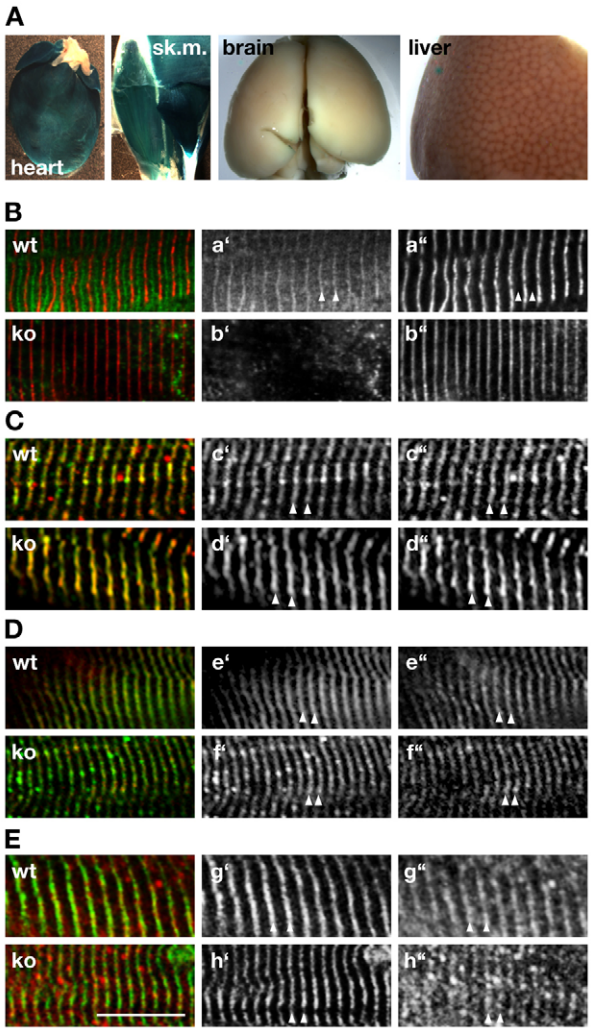

Fig. 2. Unchanged sarcomere organization in *Obscn*$^{-/-}$ mice. (A) Expression of β-galactosidase under control of the endogenous *Obscn* promoter indicates that expression of the protein is restricted to cross-striated muscles, but is markedly absent from brain and liver. (B) Endogenous Obsc is localized to the region of the sarcomeric M-band (arrowhead) in wild-type (wt), but absent in *Obscn*$^{-/-}$ (ko) muscles stained with antibodies against Obsc (Ba′,b′; green in overlay) and α-actinin (Ba″,b″; red in overlay). (C,D) Lack of Obsc in skeletal muscles derived from *Obscn*$^{-/-}$ mice has no marked effect on Z-disc structure (arrowheads in C), as concluded by antibodies against titin-Z1Z2 (Cc′,d′; green in overlay) and α-actinin (Cc″,d″; red in overlay). Judging from the staining of skeletal muscle tissues by antibodies against titin-M8 (De′,f′; green in overlay) and myomesin (De″,f′; red in overlay) the sarcomeric M-band (arrowheads in D) is also unaffected in obscurin knockouts. (E) Antibodies against Obsl1-Ig1 (Eg″,h″; red in overlay) decorate the region of the sarcomeric M-band (arrowheads) in obscurin knockout as well as wild-type muscle tissues. Myomesin (Eg′,h′; green in overlay) was the sarcomeric counterstain. Scale bar: 10 μm. All investigated muscles (B-E) were either from tibialis anterior or diaphragm.

Altered expression and localization of small ankyrin

Several ankyrin isoforms have been shown to bind to the extreme C-terminus of Obsc-A (Bagnato et al., 2003; Cunha and Mohler, 2008; Kontrogianni-Konstantopoulos et al., 2006; Kontrogianni-Konstantopoulos et al., 2003). This interaction with ankyrin membrane proteins led to the hypothesis that Obsc might regulate SR integrity and function. We employed antibodies against sAnk1.5 to study the integrity and subcellular localization of the SR in mice lacking Obsc. As demonstrated in Fig. 3A, sAnk1.5 predominantly localizes to the region of the sarcomeric M-band in wild-type controls. The localization of sAnk1.5 in *Obscn*$^{-/-}$ skeletal muscles, however, appears largely diffuse throughout the cell or hazy at the level of the sarcomeric I-band, indicating mislocalization of sAnk1.5 and/or structural changes of the longitudinal SR architecture. This

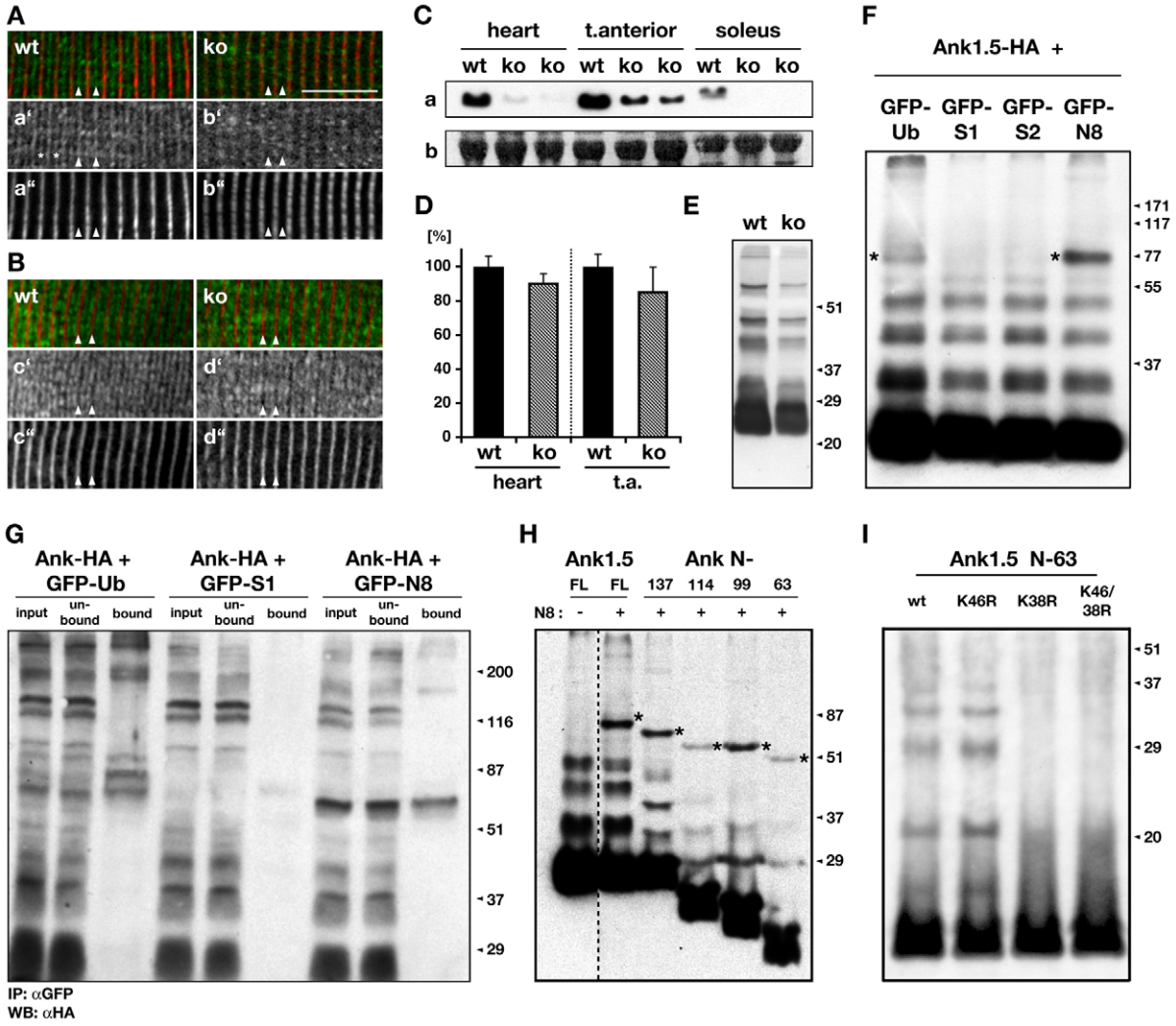

Fig. 3. Changes in sAnk1.5, and its post-translational modifications. (A) Skeletal muscles show a marked shift of the sAnk1.5 (Aa′,b′; green in overlay) localization from the sarcomeric M-band (arrowheads) in wild type (wt), to the I-band and Z-disc in *Obscn*$^{-/-}$ (ko) muscle tissue. The sarcomeric counterstain is α-actinin (Aa″,b″; red in overlay). Note the weak I-band and Z-disc staining of sAnk1.5 in wild-type tissue samples (asterisks). Scale bar: 10 µm. (B) Ryanodine receptor localization is unaffected in obscurin knockouts. No changes were found for skeletal muscles of *Obscn*$^{-/-}$ and wild-type controls that were stained with antibodies against RyR1 (Bc′,d′; green in overlay) and titin domain M8 (Bc″,d″; red in overlay). All muscles (A,B) were from diaphragm. (C) Immunoblot analysis of total protein samples from heart, tibialis anterior and soleus of *Obscn*$^{-/-}$ and wild-type controls showed marked downregulation of sAnk1.5 (a) in *Obscn*$^{-/-}$ tissues (see also supplementary material Fig. S5C). sAnk1.5 was detected at approx. 25 kDa. Ponceau-red stained actin is used as loading control (b). (D) Semiquantitative RT-PCR of heart and tibialis anterior muscles detected lower, but not significantly altered sAnk1.5 mRNA levels. Shown are mRNA levels normalized against GAPDH and arbitrarily set to 100% for the corresponding wild type. (n=4; P-values comparing wild-type and *Obscn*$^{-/-}$ heart, or tibialis anterior are P=0.29, and P=0.25, respectively). (E) Immunoblot of proteins from enriched SR vesicle fractions, prepared according to Morii et al. (Morii et al., 1985), of wild-type and *Obscn*$^{-/-}$ skeletal muscle tissue samples exhibited sAnk1.5 positive bands with higher molecular weight, indicating post-translational modification of endogenous ankyrin. Note that sAnk1.5 has been modified regardless of the origin (wt vs. ko) of the samples. (F) Modification of sAnk1.5 by Ubls. Lysates of Cos-1 cells cotransfected with Ank1.5-HA and either GFP-tagged ubiquitin (Ub), sumo1 (S1), sumo2 (S2) or nedd8 (N8) were analyzed by immunoblotting, using antibodies directed against the HA-tag. Note: additional high-molecular-weight bands in lane 1 and 4 (asterisk) correspond to ankyrin covalently modified by GFP-tagged Ubls not visible in lanes 2, 3. (G) CoIP assays using sAnk1.5-HA and either GFP-tagged ubiquitin (Ub), sumo1 (S1) or nedd8 (N8) demonstrate modification of ankyrin by ubiquitin or nedd8, but not sumo1. (H) Serial C-terminal truncation of HA-tagged ankyrin demonstrates that the minimal region sufficient for the modification of sAnk1.5 by GFP-nedd8 is located within the first 63 N-terminal residues. Asterisks mark sAnk1.5 covalently modified by GFP-nedd8 (N8). (I) Site-specific mutagenesis of HA-tagged truncated sAnk1.5 (residues 1-63). K38R abrogates modification by endogenous Ubls, whereas mutagenesis of K46R has no effect. Note that full-length Ank1.5 K38R still displays post-translational modification of the protein (not shown), indicating that other C-terminal lysine residues can substitute. All marker values are in kDa.

Journal of Cell Science

result supports earlier findings (Bagnato et al., 2003; Kontrogianni-Konstantopoulos et al., 2006) that the correct localization of sAnk1.5 is dependent on its interaction with obscurin and its anchorage at the sarcomeric M-band. In order to determine whether junctional SR is also affected in *Obscn*$^{-/-}$ muscles, we employed antibodies against the junctional SR protein RyR. As demonstrated in Fig. 3B no apparent changes in the localization and expression level of RyR1 was observed (supplementary material Fig. S3A). To summarize, our results suggest dramatic modifications to sAnk1.5 localization and longitudinal SR morphology with little or no alterations at the level of the junctional SR.

sAnk1.5 can be modified by nedd8 and ubiquitin

We further investigated the biological consequences of the mislocalization of sAnk1.5 in *Obscn*$^{-/-}$ muscles by asking whether sAnk1.5 expression levels were also affected. We hypothesized that a destabilization of the Obsc-sAnk1.5 protein complex induced by the absence of Obsc might lead to an increased turnover of the protein. As demonstrated in Fig. 3C (and supplementary material Fig. S3Ca), protein levels of sAnk1.5 are downregulated in *Obscn*$^{-/-}$ heart and skeletal muscles, whereas normalized sAnk1.5 mRNA levels appear not to be significantly altered (Fig. 3D). These changes suggest increased degradation of sAnk1.5 in *Obscn*$^{-/-}$ muscle tissue.

To further examine the susceptibility of sAnk1.5 to degradation, we investigated the putative modification of sAnk1.5 by ubiquitin or ubiquitin-like modifiers (Ubls). Analysis of the sAnk1.5 amino-acid sequence using *PESTFIND* yielded poor matches for two regions within the protein C-terminus (supplementary material Fig. S2A). Immunoblot analysis of enriched skeletal muscle SR-vesicle fractions displayed a typical 'ladder' effect of endogenous sAnk1.5, possibly due to post-translational modification by ubiquitin or Ubls (Fig. 3E). Coexpression of full-length sAnk1.5 with GFP-tagged ubiquitin, sumo1, sumo2 or nedd8 indicated the modification of sAnk1.5 by ubiquitin and nedd8, as demonstrated by additional high-molecular-weight bands corresponding to sAnk1.5 that was covalently modified by GFP-ubiquitin or GFP-nedd8 (Fig. 3F, asterisks lane 1, 4). The successful modification of sAnk1.5 by ubiquitin and nedd8 could also be demonstrated by co-immunoprecipitation (Fig. 3G), but again failed to substantiate a modification of sAnk1.5 by sumo. Truncation constructs of sAnk1.5 further indicated that the site sufficient for the modification by nedd8 resides in the first 63 residues (Fig. 3H). Sequence analysis of this minimal region indicated two putative lysine residues available for modification by nedd8 or ubiquitin, namely K38 and K46 (see below). Consequently, we mutated these residues to arginine in order to test for changes in the post-translational modification of sAnk1.5. As demonstrated in Fig. 3I, only sAnk1.5 (residues 1-63) mutated at residue K38 displayed a complete lack of the characteristic protein laddering that was visible in the wild type and with sAnk1.5 that had been mutated only at residue K46.

Investigation of *Obscn*$^{-/-}$ skeletal muscles for changes in localization of nedd8 and ubiquitin showed minor changes in nedd8 localization, with a more pronounced M-band staining in wild-type than in knockout muscles, and no changes in ubiquitin localization (supplementary material Fig. S2B, arrows; Fig. S2C).

We demonstrated that sAnk1.5 localization and levels of sAnk1.5 expression are altered in obscurin knockout tissues. The downregulation of sAnk1.5 occurs at the protein level, and might be due to ubiquitylation and/or neddylation of sAnk1.5.

Changes in SR-associated proteins

Besides its interaction with sAnk1.5, Obsc has recently been shown to interact with muscle-specific isoforms of Ank2. Does the absence of Obsc also result in changes to Ank2 and/or to associated proteins like spectrin or NCX1? As demonstrated in Fig. 4A, Ank2 localized mainly to the region of the junctional SR in skeletal muscle cells of both wild-type and *Obscn*$^{-/-}$ mice. In addition, no apparent changes could be found in the protein localization of the Ank2-associated proteins β-spectrin (not shown), and NCX1 (Fig. 4C), nor to SERCA or triadin (Fig. 4B; supplementary material Fig. S3D). These results corroborate our previous finding using RyR1 antibodies (Fig. 3B) that indicated changes to the longitudinal SR, but no alterations to the localization of junctional SR proteins. Analysis of the expression levels of Ank2 and β-spectrin, however, displayed increased protein levels in *Obscn*$^{-/-}$ muscle tissues (Fig. 4Da,b), but failed to show major changes in RyR1, SERCA, DHPR2 (supplementary material Fig. S3A,Cb,c) or NCX1 expression levels (not shown). An increase in Ank2 and spectrin might point towards an augmentation of junctional SR structure. However, these changes

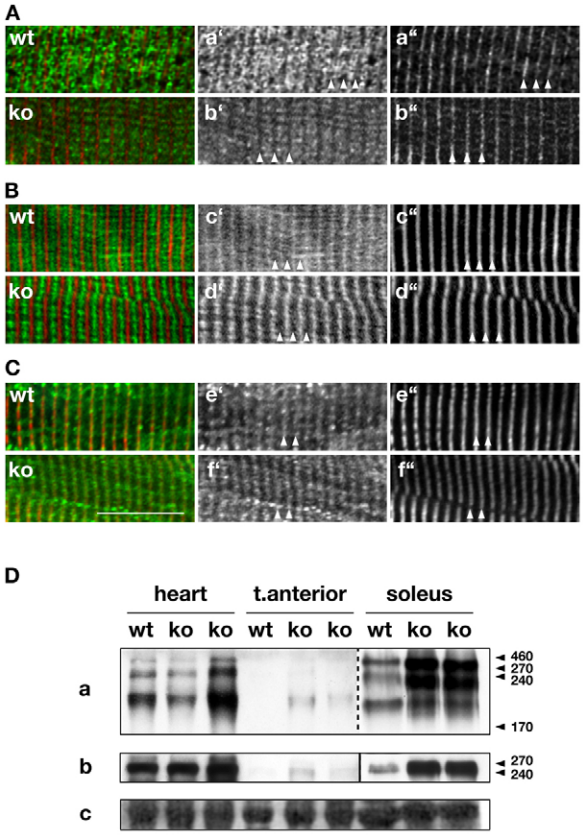

Fig. 4. Junctional SR and SR-associated proteins. (A-C) Immunohistochemistry of junctional SR proteins Ank2 (Aa′,b′), SERCA (Bc′,d′) and NCX1 (Ce′,f′) display no changes in localization between wild-type and *Obscn*$^{-/-}$ skeletal muscle cells (all green in overlays). Titin-M8 (Aa″,b″; Bc″,d″) or α-actinin (Ce″,f′) have been used as sarcomeric markers (red in overlays). Scale bar: 10 μm. All investigated muscles were from tibialis anterior or diaphragm. (D) Immunoblot analysis of heart, tibialis anterior and soleus tissue samples show marked increase of Ank2 (a) and β-spectrin (b) expression in *Obscn*$^{-/-}$ samples from all investigated tissues. Note: the image for Ank2 in soleus was taken with shorter exposure times than for other samples of the same blot. Ponceau-red-stained actin (c) is shown as loading control. Marker values are in kDa.

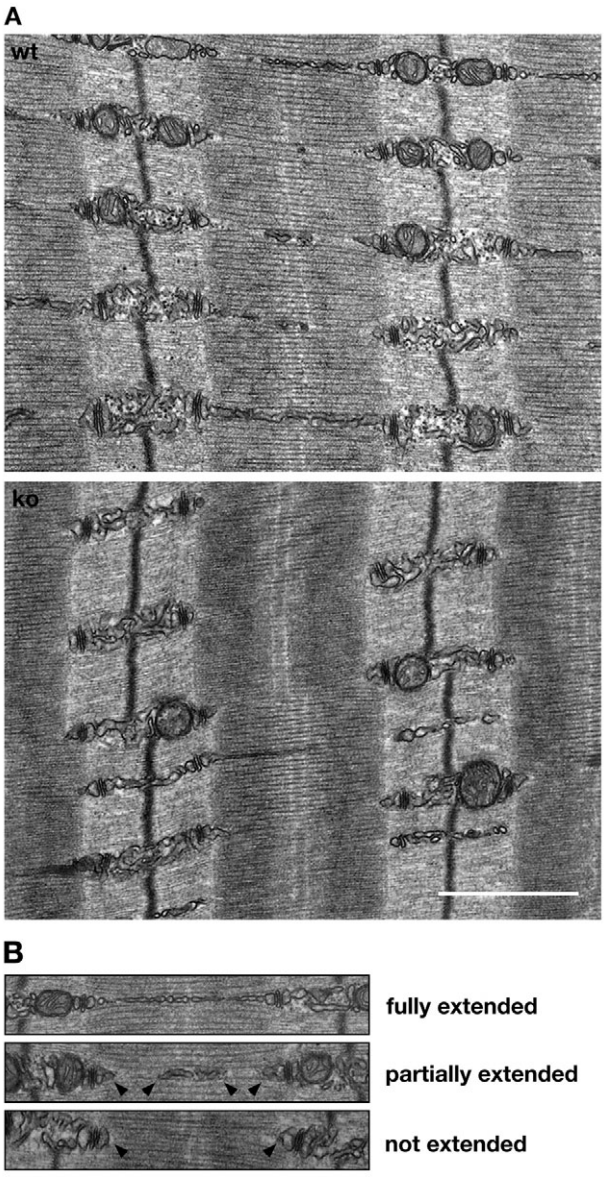

Fig. 5. Obscurin regulates longitudinal SR architecture. (A) TEM images of wild-type (wt) and *Obscn*$^{-/-}$ (ko) tibialis anterior muscle samples display normal sarcomeric structure in knockout muscles, but changes in longitudinal SR architecture. Although mitochondrial density seems to be affected in *Obscn*$^{-/-}$, results could not be corroborated using CoxIV antibodies (supplementary material Fig. S3B). Scale bar: 1 μm. (B) Longitudinal SR of wt and ko muscles were divided into three groups: fully extended, partially extended (arrowheads) and not extended (arrowheads). Whereas a majority of the wild-type longitudinal SR has been fully or partially extended over the length of the sarcomere, *Obscn*$^{-/-}$ muscle tissues display either no or only partially extended longitudinal SR. See Table 1 for quantification of the changes.

do not seem to coincide with a remodeling of the protein amount of important SR ion-channels.

Alterations in *Obscn*$^{-/-}$ SR ultrastructure

To investigate putative changes of the sarcomere and the SR at the ultrastructural level, we analyzed transmission electron microscopic (TEM) images of wild-type and *Obscn*$^{-/-}$ tibialis anterior muscles (Fig. 5A). Sarcomeres in *Obscn*$^{-/-}$ muscles appear to be unaltered. This result corroborates our earlier findings for Z-disc and M-band epitopes of the major structural proteins α-actinin, titin and myomesin. The junctional SR also displayed no significant changes between knockout and wild-type tissues (supplementary material Fig. S6A-B), validating our results using RyR antibodies. Although the cross-sectional area of T-tubules appears to be slightly increased in knockout muscles (supplementary material Fig. S6A,B), DHPR and NCX1 localization in T-tubules was unaltered at the light-microscopic level (Fig. 4C; supplementary material Fig. S3E). Closer inspection of the longitudinal SR, however, indicated changes to longitudinal SR structure (Fig. 5B). Whereas in wild-type muscles a majority (>50%) of the longitudinal SR is extended over the full length of the sarcomere, *Obscn*$^{-/-}$ muscles exhibit significantly lower values (<15%) of longitudinal SR extension (Table 1). These differences indicate a dramatic decrease in the lateral SR 'connectivity' and might point to physiological changes in muscle contraction.

No physiological changes in *Obscn*$^{-/-}$ skeletal muscle

Are these changes in SR architecture indicative of impaired physiological performance in the skeletal muscles of *Obscn*$^{-/-}$ mice? To answer this question, we investigated several parameters of the fast extensor digitorium longus (EDL) muscle architecture and physiology from *Obscn*$^{-/-}$ and wild-type littermate controls.

Dissected EDL muscles from *Obscn*$^{-/-}$ mice were similar in gross appearance to those of the wild-type littermates, but had reduced muscle mass and fiber length (Table 2). Resting sarcomere lengths and myosin heavy chain isoform compositions (not shown) were not significantly different between groups and were comparable to published values (Chleboun et al., 1997). Muscle mass and physiological cross-sectional area (PCSA) were also similar to those published previously (Chleboun et al., 1997).

Because the SR is involved in calcium release and uptake, we measured several twitch parameters. Twitch contractions did not differ significantly in any of the standard defining measurements: peak stress during twitch (PT) (left panel, Fig. 6A), time to peak tension (TPT) or half relaxation time (HRT). Force-frequency relationships for wild type and *Obscn*$^{-/-}$ were also similar, with no significant difference in the stress produced during fully fused isometric tetanus (right panel, Fig. 6A) or the half-fusion frequence (Fig. 6B). To isolate the contribution of excitation-contraction coupling to muscular stress production, caffeine was added, inducing

Table 1. Changes to longitudinal SR in *Obscn*$^{-/-}$ mice

	% of fully extended longitudinal SR	% of partially extended longitudinal SR	% of not extended longitudinal SR
Wild type (*n*=307)	53.4±6.2	31.3±4.4	15.4±5.1
Knockout (*n*=204)	14.7±5.1*	29.7±5.5	55.7±9.2*

Quantification of changes to longitudinal SR architecture, scored as shown in Fig. 5B. Two wild-type and two *Obscn*$^{-/-}$ animals with 26 cells in each group were statistically analyzed; *n* values and standard errors are shown; *P<0.01, wild-type vs knockout animals.

Journal of Cell Science

release of calcium from the SR. Twitch and titanic potentiation following caffeine addition were not significantly different between wild type and *Obscn*$^{-/-}$ (Table 2). To summarize, we found no significant alterations in EDL performance between *Obscn*$^{-/-}$ and wild-type controls. Apparent changes that are visible to SR architecture and protein composition at the microscopic scale do not directly translate to functional changes of the muscle.

Centralized nuclei in aged *Obscn*$^{-/-}$ skeletal muscle

One of the hallmarks of muscular dystrophies is the occurrence of centralized nuclei in skeletal muscle cross-sections (Briguet et al., 2004). Obsc and Obsl1 have recently been linked to the LGMD2J-type muscular dystrophy (Hackman et al., 2002; Udd et al., 2005), whereby mutations in the C-terminal titin domain M10 weaken or abrogate the interaction of titin to Obsc and/or Obsl1 (Fukuzawa et al., 2008). Therefore, we asked whether ablation of Obsc results in centralized skeletal muscle nuclei and abrogates the localization and expression of the calpain p94, effects that are reminiscent of this type of muscular dystrophy in humans.

Cross-sections of whole legs were stained with DAPI and a laminin antibody in order to determine nuclei localization within muscle fibers (Fig. 6C). Quantification of wild-type and *Obscn*$^{-/-}$ tibialis anterior muscles of four different age-stages showed a significant increase of centralized nuclei in *Obscn*$^{-/-}$ muscles after 12 months of age (Fig. 6D).

In contrast to the centralized nuclei phenotype present in the *Obscn*$^{-/-}$ animals, analysis of calpain p94 expression levels (Fig. 6E) and its subcellular localization showed no difference between knockout and wild-type controls (Fig. 6F). Taken together, the centralized nuclei in aged animals indicate a mild skeletal myopathy in *Obscn*$^{-/-}$ mice. The lack of C-terminal titin domains as well as the absent calpain p94 staining from human patients, which are hallmarks of the recently described and obscurin-linked LGMD2J phenotype (Hackman et al., 2002), are not mirrored in our animal model and might indicate redundant functions of other proteins like Obsl1 that compensate for the loss of Obsc.

Discussion

The biological functions of obscurin remained enigmatic for some time. Its discovery as a binding partner for Z-disc domains of titin (Bang et al., 2001; Young et al., 2001) did not match its localization in cross-striated muscle fibers. Although the complex splicing pattern of obscurin (Fukuzawa et al., 2005) might account for its sometimes variable localization pattern (Bowman et al., 2007; Carlsson et al., 2008), it was not until recently that the dominant sarcomeric M-band binding partners for Obsc have been identified as titin domain M10 and myomesin (Fukuzawa et al., 2008). Mutations in Obsc and its binding partners have been linked to hypertrophic cardiomyopathies (Arimura et al., 2007) as well as LGMD2J (Fukuzawa et al., 2008), highlighting the biological importance of the protein for proper myofibrillogenesis and muscle maintenance.

We investigated Obsc function by establishing an obscurin knockout mouse and analyzed the effect of the lack of Obsc on its interaction partners such as ankyrin, on the SR architecture, on the subcellular localization and altered expression of SR-associated proteins, and on muscle physiology. Despite identifying only a mild physiological phenotype, we found major changes in *Obscn*$^{-/-}$ muscle tissues that occurred at the longitudinal SR and affected the expression and localization of SR-associated proteins.

Obscurin

Although previous reports indicated that obscurin might play an important role for myofibrillogenesis and myofibril alignment (Borisov et al., 2006; Bowman et al., 2008; Raeker et al., 2006), we found that proteins important for the structure of the sarcomere (like α-actinin, Z-disc and M-band epitopes of titin, and myomesin) are unaffected by the lack of obscurin. Our TEM analysis showed preserved sarcomere organization and alignment, substantiating our immunohistological findings. A recent report (Fukuzawa et al., 2008) proved that the N-terminal Ig-domain of Obsl1 exhibits functional redundancy for the sarcomeric interactions of Obsc with myomesin and the C-terminal titin domain M10, suggesting that Obsl1 might functionally compensate for the sarcomeric functions of obscurin. It would be interesting to see how a loss of both obscurin and Obsl1 might affect muscle formation and maintenance.

Several proteins have been identified as binding to the signaling domains in obscurin (Fig. 1D): calmodulin binds to the IQ-motif (Young et al., 2001), RanBP9 binds to the obscurin DH-domain (Bowman et al., 2008), and the novel protein phosphatase scpl-1 interacts with the putative kinase domains in the *C. elegans* unc-89 homolog of obscurin (Qadota et al., 2008). Calmodulin localization was not altered in *Obscn*$^{-/-}$ skeletal muscle tissues (not shown).

The interaction of the obscurin DH-domain with RanBP9 was found to regulate titin Z-disc assembly (Bowman et al., 2008). Examination of sarcomerogenesis and of Z-disc and sarcomere structure in *Obscn*$^{-/-}$ animals, however, displayed no differences between *Obscn*$^{-/-}$ and control muscles. The overexpression of obscurin fragments and/or RanBP9 can be more apprehended as a

Table 2. EDL muscle architectural parameters and contractile properties

	4-month-old animals		1-year-old animals	
Parameters	wt	*Obscn*$^{-/-}$	wt	*Obscn*$^{-/-}$
Resting sarcomere length	2.35±0.05 μm	2.33±0.03 μm	2.30±0.07 μm	2.14±0.22 μm
Muscle length	9.00±0.24 mm	9.06±0.20 mm	9.91±0.18 mm	9.64±0.29 mm
Fiber lengths	**6.94±0.19 mm**	**6.31±0.32 mm**	**7.25±0.24 mm**	**6.17±0.1 mm**
Muscle mass	3.65±0.16 mg	3.43±0.12 mg	**5.37±0.32 mg**	**4.27±0.12 mg**
PCSA (physiological cross sectional area)	0.49±0.02 mm^2	0.51±0.01 mm^2	0.69±0.05 mm^2	0.64±0.01 mm^2
PT (peak tension)	54.5±5.6 kPa	50.5±4.4 kPa	48.5±5.1 kPa	57.4±7.9 kPa
TPT (time to peak tension)	21.78±0.83 ms	25.27±1.33 ms	23.57±2.49 ms	23.43±2.89 ms
HRT (half relaxation time)	22.85±1.27 ms	26.07±3.05 ms	22.33±3.18 ms	30.33±1.69 ms
Twitch potentiation	60.0±3.9%	64.4±5.0%	48.8±16.1%	47.4±12.9%
Stress during tetanus	217±14 kPa	207±27 kPa	154±8 kPa	184±23 kPa
Half-fused tetanus	29.52±2.09 Hz	30.92±3.23 Hz	31.63±8.93 Hz	30.66±7.27 Hz

Obscurin knockout display with decreased EDL fiber length and muscle mass signs for a mild myopathy. Results are means ± s.e.m. (n=6 for 4-month-old animals, n=3 for 1-year-old animals). Values in bold are those showing a significant difference between wt and *Obscn*$^{-/-}$, with P<0.05.

'gain-of-function' model that might induce secondary effects not typically seen in vivo, which in turn affect sarcomere assembly. Our 'loss-of-function' animal model might not reproduce the described overexpression effect of obscurin fragments and/or RanBP9 on sarcomere formation and the disruption of titin Z-disc organization.

Our *Obscn*$^{-/-}$ animal model is also somewhat restricted as a model to probe for obscurin kinase functions, because the putative 'kinase-only' *KIAA1639* is not ablated in our *Obscn*$^{-/-}$ mice. Indeed, RT-PCR analysis demonstrates the persistent presence of *KIAA1639* mRNA in *Obscn*$^{-/-}$ muscle tissues (supplementary material Fig. S1Bf,g). Furthermore, putative small Obsc splice variants circumventing coding exon 1 might exist, but could not be detected by RT-PCR or immunoblot analysis using the ObscIQ-64 antibody (supplementary material Fig. S1Ba-e; Fig. S1C). Although RT-PCR was unsupportive of the existence of Obsc 'Mini-A', immunoblot results with a different antibody (Obsc66/67) displayed weak cross-reactivity in heart and skeletal muscles (supplementary material Fig. S1D), leaving the possibility open for small Obsc isoforms (<200 kDa). However, because the data so far do not firmly establish the expression of small obscurin isoforms in the knockout, we suggest that *KIAA1639* might represent the only obscurin gene product not directly affected by our knockout strategy.

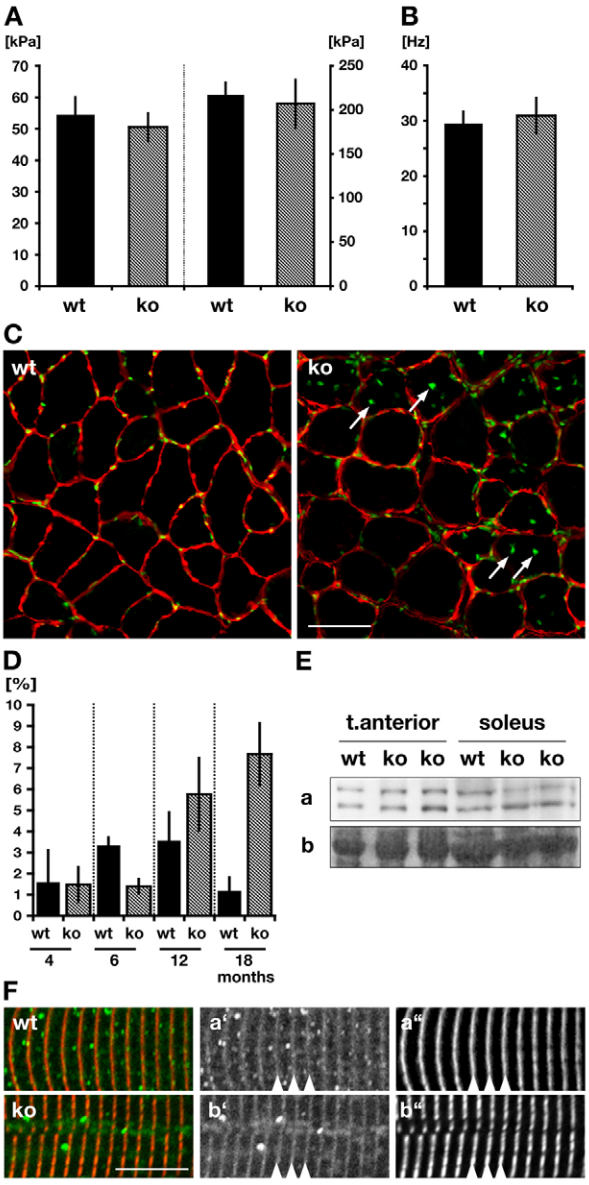

Fig. 6. Muscle physiology and myopathy in *Obscn*$^{-/-}$ mice. (A,B) Peak tension during twitch (left panel in A) and stress during peak tetanus (right panel in A) as well as half-fused tetanus frequency (B) measurements display no significant changes between wild-type (wt) and *Obscn*$^{-/-}$ (ko) EDL muscles. (C) Immunohistochemistry of tibialis anterior muscle cross-sections stained with laminin antibodies (red) and DAPI (green) shows marked increase of centralized nuclei (arrows) in *Obscn*$^{-/-}$ when compared to wild types. Scale bar: 50 µm. (D) Quantification of C for different developmental stages indicates age-dependent occurrence of fibers that contain centralized nuclei (in %) in *Obscn*$^{-/-}$. (E,F) Analysis of the level of expression of calpain p94 (Ea) and its localization (Fa′,b′; green in overlay) in skeletal muscles displays no difference between *Obscn*$^{-/-}$ and wild-type muscles. Sarcomeric marker was titin M8 (Fa″,b″; red in overlay). Ponceau-red-stained actin (Eb) is shown as loading control.

In contrast to our findings, several reports using RNAi techniques in rat skeletal myotubes and cardiomyocytes (Borisov et al., 2006; Kontrogianni-Konstantopoulos et al., 2006), zebrafish (Raeker et al., 2006) and *C. elegans* (Small et al., 2004) suggested that Obsc might be essential for sarcomere formation and lateral alignment of the myofibrils. Comparing the effects of RNAi in non-vertebrate cells with a vertebrate knockout model is difficult. Unc89, the *C. elegans* equivalent of obscurin displays a somewhat divergent domain layout compared with vertebrate and mammalian obscurin proteins. Gene duplication events during evolution resulted in two *obsl1* and two *obsc* genes in zebrafish (Geisler et al., 2007; Raeker et al., 2006). Discrepancies between our findings and those studies could also reflect differences in the systems being used: gene deletion versus RNAi; mouse versus zebrafish or rat; in vivo versus in vitro.

Ankyrin

The most pronounced effects observed in the *Obscn*$^{-/-}$ mice are changes in ankyrin proteins and in the SR architecture (Fig. 7A). Two different ankyrins have been shown to interact with the C-terminal region of Obsc-A and are thought to link Obsc to the SR. The best investigated among these ankyrins is the muscle-specific isoform sAnk1.5, which is thought to form an integral part of the SR membrane with its trans-membrane domain (Bagnato et al., 2003; Borzok et al., 2007). Our experiments clearly indicate that correct sAnk1.5 localization in vivo depends on its interaction with obscurin, which is in agreement with earlier publications (Bagnato et al., 2003; Kontrogianni-Konstantopoulos et al., 2006; Kontrogianni-Konstantopoulos et al., 2003). Moreover, we found that TEM images of *Obscn*$^{-/-}$ muscles displayed insufficient longitudinal SR membrane structures that extend over the A-band of the sarcomere. We concluded that the lack of correct anchorage of sAnk1.5 at the M-band results in an impairment of the correct development of longitudinal SR architecture in muscle tissues of *Obscn*$^{-/-}$ (Fig. 7A, lower panel). However, proteins that are anchored at the junctional SR displayed no dramatic alterations in *Obscn*$^{-/-}$ muscles, indicating that SR architecture was mostly affected on the level of the longitudinal SR membrane. Although the cross-sectional area of T-tubules increased slightly in the knockouts, a dramatic SR-phenotype like that observed in other mouse models (Knollmann et al., 2006) was not evident in *Obscn*$^{-/-}$ muscle. Ultimately, computer tomography and three-dimensional reconstruction is required to determine the precise extent of changes to the SR and other membrane systems in obscurin knockout muscle.

Ankyrin-2 has also been implicated to be of outmost importance for SR architecture and protein localization (Mohler et al., 2002).

Moreover, muscle-specific isoforms of Ank2 have been recently shown to interact with Obsc-A (Cunha and Mohler, 2008). These Ank2 isoforms share two evolutionarily conserved obscurin-binding domains (OBDs) with sAnk1.5. Although, in our hands, Ank2 localization was restricted to the junctional SR and did not change in *Obscn*$^{-/-}$, we did see changes in Ank2 expression levels in muscles of *Obscn*$^{-/-}$ mice. The increased expression of Ank2 and β-spectrin, an ankyrin-binding protein, was not mirrored with variations in the expression levels or localizations of ion-channels like RyR1, SERCA, DHPR (supplementary material Fig. S3A,Cb,c,E) or NCX1 (not shown), indicating a reinforcement of components important for junctional SR structure, rather than changes to channel functions.

Ankyrin and ubiquitin-like modifiers

Apart from the pronounced misclocalization of sAnk1.5 in mice that lack obscurin, we noticed a significant downregulation of the protein in muscle tissues of these mice. We found that sAnk1.5 downregulation is not caused by decreased mRNA levels in the knockout mice, but rather occurs on the protein level. The most prominent mechanism for the proteolytic system in cells is the 'ubiquitin-proteasome system' (UPS). In fact, we found that concentrated SR-vesicle fractions of wild-type and *Obscn*$^{-/-}$ muscle tissues displayed ankyrin bands with higher than expected molecular weights – in other words, a typical protein 'laddering' effect indicative of post-translational modification of sAnk1.5 by ubiquitin or Ubls. Earlier publications attributed the occurrence of high-molecular-weight sAnk1.5 bands to oligomerization of the protein by disulfide bridges (Porter et al., 2005). However, our experiments indicate that some of these bands might represent post-translationally modified sAnk1.5, as also seen by sAnk1.5 that is devoid of all cysteine residues, which are needed for formation of disulfide bridges (supplementary material Fig. S2D).

The giant isoforms of ankyrin-1 have been shown to be a substrate of the ubiquitin E3-ligase activity of spectrin (Hsu and Goodman, 2005). The muscle-specific sAnk1.5, however, lacks the spectrin-binding domain and all of the ankyrin motifs identified to be modified by ubiquitin (Chang et al., 2004). Nevertheless, our tests demonstrate that ubiquitin and nedd8 are post-translational modifiers of sAnk1.5. Very few substrates for the neddylation machinery have been identified, like the cullin proteins (Pan et al., 2004), EGFR (Oved et al., 2006) and p53 (Xirodimas et al., 2004), making sAnk1.5 a novel substrate for the modification by nedd8. The minimal region necessary for the post-translational modification includes the first 63 residues of sAnk1.5, with lysine K38 being important for attachment of the Ubls. Neddylation has been demonstrated to enhance the ubiquitylation of substrates by aiding the positioning of the E2 complex (Oved et al., 2006; Pan et al., 2004). Preliminary data acquired during the search for further sAnk1.5 interaction partners indicate that a complex of adaptor proteins might assist the neddylation and ubiquitylation of the protein (not shown). Further analysis of sAnk1.5 and its interactors might give intriguing insights into the complex system of SR protein turnover.

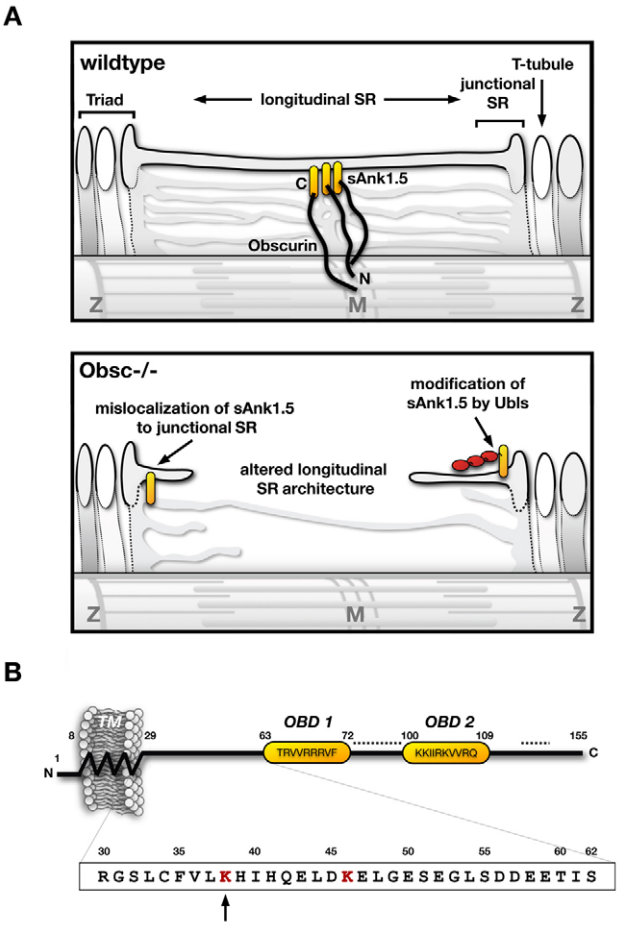

Fig. 7. Model of changes in *Obscn*$^{-/-}$ muscles and sAnk1.5 domain layout. (A) Model for the alterations in skeletal muscle longitudinal SR architecture and sAnk1.5 protein levels in *Obscn*$^{-/-}$ mice. Mislocalization of sAnk1.5 and modification by Ubls (in red) are indicated. (B) Layout of the sAnk1.5 protein. The N-terminal transmembrane domain (TM), and the two obscurin-binding domains (OBD) are marked. Residue numbers note the boundaries of each motif. Dashed lines indicate putative PEST motifs (supplementary material Fig. S2A). Residues in the box indicate the minimal cytoplasmic region sufficient for modification by Ubls, with lysines in red and K38 marked by the arrow.

Obscurin-linked myopathies

Two reports implicate a direct or indirect role for obscurin in the development of hereditary cardiac (Arimura et al., 2007) or skeletal muscle myopathies in man (Fukuzawa et al., 2008). Preliminary results indicate that the hearts of our *Obscn*$^{-/-}$ mice do not show any signs of cardiomyopathy (not shown). In this report we investigated several markers indicative of muscular dystrophies. However, we were only able to identify one marker to be present in skeletal muscles of *Obscn*$^{-/-}$ mice, namely elevated levels of centralized nuclei in older *Obscn*$^{-/-}$ mice. Loss of calpain p94 and the C-terminal titin epitopes that are characteristic of the LGMD2J phenotype (Hackman et al., 2002; Udd et al., 2005) were absent in our animal model. Functional redundancy between the N-terminal domains of Obsl1 and Obsc might account for the lack of a clear dystrophic phenotype. The generation of mice that lack both Obsc and Obsl1 might give an answer to this question.

Materials and Methods

Generation of DNA constructs for expression

Hemagglutinin (HA)- and green fluorescent protein (GFP)-tagged constructs were essentially generated as described in Lange et al. (Lange et al., 2002). In short, the coding sequence of human sANK1.5 (NCBI acc-no: NM_020478) was subcloned to a eukaryotic expression vector, merging ankyrin to a C-terminal HA tag. The coding sequence of mouse ubiquitin, human Sumo1, Sumo2 and Nedd8 were generated by PCR from cDNA libraries and subcloned to pEGFP-C1 (Clontech) to produce an in-frame fusion between GFP and the insert.

Site-directed mutagenesis of sAnk1.5 K38R, K46R, C22G, C34G was performed as described in Fukuzawa et al. (Fukuzawa et al., 2008) using primers shown in supplementary material Table S1. All expression constructs were sequenced to determine correct integration into the vector.

Journal of Cell Science

Gene targeting and generation of *Obscn*$^{-/-}$ mouse

The obscurin gene-targeting construct was generated by subcloning isogenic 129svj genomic DNA fragments surrounding coding exon 1 of the murine obscurin gene into a targeting vector (Zhou et al., 2001), whereby a *lacZ*, *GFP* and pGK-*neomycine* gene-cassette effectively replace exon 1. The linearised construct was electroporated into R1 embryonic stem cells. Genomic DNA of G418 resistant clones were screened for homologous recombination using Southern blot analysis and a probe as indicated in Fig. 1A. Germline transmission by chimeric males was tested by agouti coat phenotype of 129-derived ES-cells. Primers to determine the genotype of the animals are shown in supplementary material Table S1.

Xgal staining of mouse tissue

For whole-mount *lacZ* expression analysis, tissue samples of *Obscn*$^{-/-}$ mice were fixed and stained using Xgal and standard staining procedure as described in Zhou et al. (Zhou et al., 2001).

Transmission electron microscopy

For TEM, mice were injected with heparin (0.5 ml, 100 U/ml), anaesthetized with Nembutal, and subsequently perfused through the left ventricle with 30 mM KCl solution, followed by fixative (2% paraformaldehyde, 2% glutaraldehyde in 0.15 M sodium cacodylate buffer, pH 7.4). The muscles were dissected out, cut into smaller pieces, and kept in fixative for 4 hours. Tissue was post-fixed with 1% OsO_4, 0.8% potassium ferrocyanide in 0.15 M sodium cacodylate buffer overnight. The following day, tissue was stained for 2 hours in 2% uranyl acetate, dehydrated, and embedded into Durcupan resin (EMD, Gibbstown, NJ) using a standard method. Ultra-thin sections (60-70 nm) were stained with uranyl acetate and lead citrate solution, and observed with a JEOL-1200EX transmission electron microscope at an accelerating voltage of 80 kV.

Semi-quantitative RT-PCR

Total RNA of various muscle tissues was isolated using Trizol (Invitrogen) according to the instructions of the manufacturer. RNA amounts were measured with a photospectrometer (Biorad) and equalized. Reverse transcriptase reaction was performed using oligo dT_{17} primer and the Omniscript enzyme (Qiagen). Amplification of sAnk and GAPDH for standardization was done using Flexi Taq-polymerase (Promega). Bands were analyzed by agarose gel electrophoresis and quantified by densitometry using ImageJ (NIH) and Excel for statistical analysis.

Cell culture, transfection and co-immunoprecipitation

Cos-1 or C2C12 cells were transfected with eukaryotic expression constructs using Escort IV (Sigma) or Lipofectamine 2000 (Invitrogen) according to the manufacturers instructions. Cos-1 cells were harvested 48 hours after transfection and lysed either directly in SDS sample buffer (3.7 M urea, 134.6 mM Tris-HCl, pH 6.8, 5.4% SDS, 2.3% NP-40, 4.45% β-mercaptoethanol, 4% glycerol and 6 mg/100 ml bromophenol blue) or in ice-cold IP-buffer [100 mM NaCl, 10 mM Tris-HCl, pH 8, 1× Complete Protease Inhibitor Cocktail (Roche), 5 μM lactacystein, 20 mM iodoacetamide, 1 mM DTT and 0.5% NP-40]. Transfected C2C12 cells were allowed to differentiate for 2 weeks prior to cell lysis using IP-buffer. Following sonication (Sonics Vibra Cell) and separation of insoluble material by centrifugation, GFP- or HA-antibodies (Roche) were added to the lysates and the samples were incubated for more than 2 hours at 4°C to allow for immunocomplex formation. Following the addition of protein-G Sepharose to the samples and incubation for an additional hour at 4°C, beads were washed four times with ice-cold IP-buffer.

For co-immunoprecipitation (CoIP), proteins in the supernatant (unbound), proteins retained on the beads after washing (bound) as well as a sample representing all proteins prior to immunoprecipitation (input) were separated on SDS-PAGE and transferred onto nitrocellulose membranes (Schleicher-Schuell, Keene, NH) following standard procedures. Blots were stained with Ponceau (Sigma), blocked with 5% milk and sheep serum in low salt solution (9% NaCl, 10 mM Tris-HCl, pH 7.4, 0.1% Tween-20) and decorated with GFP- or HA-tag antibodies (Roche) and subsequently with a secondary HRP-conjugated antibody (DAKO). Detection was performed using an ECL system (Amersham) and X-ray films (Fuji).

SDS-agarose protein gel

Analysis of the level of expression of high-molecular-weight proteins like obscurin or RyR was done using vertical agarose gel electrophoresis (VAGE) as described (Warren et al., 2003). In short, muscle tissue was freeze homogenized as described (Lange et al., 2002) in 1:40 (sample:buffer) volumes of agarose-sample buffer (8 M urea, 2 M thiourea, 3% SDS, 75 mM DTT, 50 mM Tris-HCl, pH 6.8). Separation of proteins was done using 1% agarose gels (384 mM glycine, 30% glycerol, 0.1% SDS, 50 mM Tris-HCl, pH 8.8), following immunoblotting as described earlier.

Immunostaining and confocal microscopy

Cryosections, or whole mounts of tibialis anterior, soleus or diaphragm muscles were fixed with pre-chilled acetone for 5 minutes at –20°C, or with 4% PFA for 30 minutes at room temperature, respectively. Subsequently tissues were permeabilized with 0.2% Triton-X100 in PBS for 5-30 minutes and blocked with 1% BSA fraction V (Sigma) and 5% sheep serum in gold-buffer (155 mM NaCl, 2 mM EGTA, 2 mM $MgCl_2$, 20 mM Tris-HCl, pH 7.5) for 30 minutes. The samples were incubated with primary antibody in gold-buffer for 1 hour at room temperature or over-night at 4°C. Following three washes with PBS for 5 minutes, samples were incubated for 1 hour at room temperature with a mixture of secondary antibodies. After washing with PBS (three times, 5 minutes), samples were mounted with fluorescent mounting medium (DAKO) on glass slides and covered with cover slips.

Tissue preparations were imaged using an OLYMPUS Fluoview confocal microscope in sequential scanning mode using a 40× or 60× oil immersion objective and instrument zoom rates between 1× and 4×.

Antibodies

The polyclonal rabbit antibodies raised against epitopes in Obsc domains IQ-Ig64 and Ig66/67 (Fig. 1D) were generated in our laboratory. The following mouse, rat, rabbit and goat antibodies were used in this study: myomesin-B4 (generous gift of J. C. Perriard, ETH Zurich, Zurich, Switzerland), RyR1 (Abcam), α-actinin EA53 (Sigma), titin-Z1Z2 (generous gift of Carol Gregorio, University of Arizona, Tuscon, AZ), titin M8 (generous gift of Mathias Gautel, King's College London, UK), obsl1 Ig1 (Fukuzawa et al., 2008), sAnk1.5 (supplementary material Fig. S5) (ankyrin1 ARP42566_T100; Aviva Sysbio, San Diego, CA), GFP (Roche), HA (Roche), SERCA (Santa Cruz Biotechnology), NCX1 (Santa Cruz Biotechnology), DHPR (Abcam), nedd8 (Sigma), ubiquitin (Sigma), laminin (Abcam), ankyrin-2 (Santa Cruz Biotechnology), β-spectrin (Santa Cruz Biotechnology), calpain p94 (Abcam), CoxIV (Cell Signaling Technology), triadin (developed by K. P. Campbell, DSHB University of Iowa, IA). All fluorescent secondary antibodies were from Jackson ImmunoResearch (West Grove, PA).

Sequence analysis

Analysis of protein sequences for PEST signals was performed using the PESTFIND program (http://bips.u-strasbg.fr/EMBOSS).

Muscle preparation for physiological experiments

Experiments were performed on the fifth toe of the extensor digitorum longus (EDL) muscle of 4-month-old wild-type and obscurin knockout mice (six per group). This muscle was chosen due to its distinct origin and insertion tendons, uniform fiber length and mixed fiber type distribution (Chleboun et al., 1997). Muscles were dissected, mounted and stimulated as previously described (Sam et al., 2000). Measurements of peak tension (PT), the time from stimulation to peak tension (TPT) and time from peak tension to half relaxation (HRT) were recorded during twitch contraction. Isometric force records were obtained by applying a 400 millisecond train of 0.3 millisecond pulses at frequencies of 5, 10, 20, 30, 40, 50, 60, 80 and 100 Hz with a two minute rest between contractions. The half-fusion frequency was determined by fitting a Hill curve (Eq. 1) to the force-frequency data and calculating the frequency at which the force reaches half the maximum (fused tetanus):

$$F = \frac{freq^n}{b + freq^n}. \quad (1)$$

The bath was then exchanged for Ringers solution plus 10 mM caffeine. The effect of caffeine was evaluated by recording twitch contractions at 2-minute intervals for 10 minutes followed by three tetanic contractions. Twitch and tetanic potentiation were calculated as the percentage increase in force from Ringers solution to the maximum recorded during caffeine treatment. The experiment was synchronized and recorded by an acquisition program written in LabVIEW (National Instruments, Austin, TX) used with a data acquisition board (DAQCard-6025, National Instruments).

Following testing, muscles were cut away from their tendons and weighed. Muscle stress was calculated by normalizing muscle force to muscle physiological cross-sectional area (PCSA, Eq. 2), calculated by using the equations provided by Sacks and Roy (Sacks and Roy, 1982) and assuming a muscle density (ρ) of 1.056 g/cm^3 (Mendez and Keys, 1960):

$$PCSA = \frac{Muscle\ mass \cdot \cos(\theta)}{\rho \cdot Fiber\ length}. \quad (2)$$

Statistical analysis

Significance was determined using a one-way analysis of variance (ANOVA) calculation with a significance level of 0.05. Results are presented as means ± standard error. Number of measurements (n) and P-values are shown in the figure or legend.

We are grateful for the provision of the titin-Z1Z2 antibody by Carol Gregorio (University of Arizona) and would like to acknowledge Mathias Gautel (King's College London) for providing the titin-M8 antibody. We would like to thank Shannon Bremner, Patrick Lee and Phildrich Teh for their technical expertise and assistance, and Mathias Gautel, Elisabeth Ehler (King's College London), Andrea Domenighetti and Farah Sheikh (UCSD, CA) for constructive comments. The work is funded by grants from the NIH (J.C., R.L.L.), MDA (J.C., S.L.), AHA (K.O.) and the VA Center (R.L.L., G.M.). Deposited in PMC for release after 12 months.

Journal of Cell Science

References

Arimura, T., Matsumoto, Y., Okazaki, O., Hayashi, T., Takahashi, M., Inagaki, N., Hinohara, K., Ashizawa, N., Yano, K. and Kimura, A. (2007). Structural analysis of obscurin gene in hypertrophic cardiomyopathy. *Biochem. Biophys. Res. Commun.* **362**, 281-287.

Bagnato, P., Barone, V., Giacomello, E., Rossi, D. and Sorrentino, V. (2003). Binding of an ankyrin-1 isoform to obscurin suggests a molecular link between the sarcoplasmic reticulum and myofibrils in striated muscles. *J. Cell Biol.* **160**, 245-253.

Bang, M. L., Centner, T., Fornoff, F., Geach, A. J., Gotthardt, M., McNabb, M., Witt, C. C., Labeit, D., Gregorio, C. C., Granzier, H. et al. (2001). The complete gene sequence of titin, expression of an unusual approximately 700-kDa titin isoform, and its interaction with obscurin identify a novel Z-line to I-band linking system. *Circ. Res.* **89**, 1065-1072.

Bennett, V. and Chen, L. (2001). Ankyrins and cellular targeting of diverse membrane proteins to physiological sites. *Curr. Opin. Cell Biol.* **13**, 61-67.

Borisov, A. B., Sutter, S. B., Kontrogianni-Konstantopoulos, A., Bloch, R. J., Westfall, M. V. and Russell, M. W. (2006). Essential role of obscurin in cardiac myofibrillogenesis and hypertrophic response: evidence from small interfering RNA-mediated gene silencing. *Histochem. Cell Biol.* **125**, 227-238.

Borisov, A. B., Raeker, M. O. and Russell, M. W. (2008). Developmental expression and differential cellular localization of obscurin and obscurin-associated kinase in cardiac muscle cells. *J. Cell Biochem.* **103**, 1621-1635.

Borzok, M. A., Catino, D. H., Nicholson, J. D., Kontrogianni-Konstantopoulos, A. and Bloch, R. J. (2007). Mapping the binding site on small ankyrin 1 for obscurin. *J. Biol. Chem.* **282**, 32384-32396.

Bowman, A. L., Kontrogianni-Konstantopoulos, A., Hirsch, S. S., Geisler, S. B., Gonzalez-Serratos, H., Russell, M. W. and Bloch, R. J. (2007). Different obscurin isoforms localize to distinct sites at sarcomeres. *FEBS Lett.* **581**, 1549-1554.

Bowman, A. L., Catino, D. H., Strong, J. C., Randall, W. R., Kontrogianni-Konstantopoulos, A. and Bloch, R. J. (2008). The rho-guanine nucleotide exchange factor domain of obscurin regulates assembly of titin at the Z-disk through interactions with Ran binding protein 9. *Mol. Biol. Cell* **19**, 3782-3792.

Briguet, A., Courdier-Fruh, I., Foster, M., Meier, T. and Magyar, J. P. (2004). Histological parameters for the quantitative assessment of muscular dystrophy in the mdx-mouse. *Neuromuscul. Disord.* **14**, 675-682.

Carlsson, L., Yu, J. G. and Thornell, L. E. (2008). New aspects of obscurin in human striated muscles. *Histochem. Cell Biol.* **130**, 91-103.

Chang, T. L., Cubillos, F. F., Kakhniashvili, D. G. and Goodman, S. R. (2004). Ankyrin is a target of spectrin's E2/E3 ubiquitin-conjugating/ligating activity. *Cell Mol. Biol.* **50**, 59-66.

Chleboun, G. S., Patel, T. J. and Lieber, R. L. (1997). Skeletal muscle architecture and fiber-type distribution with the multiple bellies of the mouse extensor digitorum longus muscle. *Acta Anat. (Basel)* **159**, 147-155.

Clark, K. A., McElhinny, A. S., Beckerle, M. C. and Gregorio, C. C. (2002). Striated muscle cytoarchitecture: an intricate web of form and function. *Annu. Rev. Cell Dev. Biol.* **18**, 637-706.

Cunha, S. R. and Mohler, P. J. (2006). Cardiac ankyrins: essential components for development and maintenance of excitable membrane domains in heart. *Cardiovasc. Res.* **71**, 22-29.

Cunha, S. R. and Mohler, P. J. (2008). Obscurin targets ankyrin-B and protein phosphatase 2A to the cardiac M-line. *J. Biol. Chem.* **283**, 31968-31980.

Dalen, H., Odegarden, S. and Saetersdal, T. (1987). The application of various electron microscopic techniques for ultrastructural characterization of the human papillary heart muscle cell in biopsy material. *Virchows Arch. A Pathol. Anat. Histopathol.* **410**, 265-279.

Fukuzawa, A., Idowu, S. and Gautel, M. (2005). Complete human gene structure of obscurin: implications for isoform generation by differential splicing. *J. Muscle Res. Cell Motil.* **26**, 427-434.

Fukuzawa, A., Lange, S., Holt, M., Vihola, A., Carmignac, V., Ferreiro, A., Udd, B. and Gautel, M. (2008). Interactions with titin and myomesin target obscurin and obscurin-like 1 to the M-band: implications for hereditary myopathies. *J. Cell Sci.* **121**, 1841-1851.

Gallagher, P. G. and Forget, B. G. (1998). An alternate promoter directs expression of a truncated, muscle-specific isoform of the human ankyrin 1 gene. *J. Biol. Chem.* **273**, 1339-1348.

Geisler, S. B., Robinson, D., Hauringa, M., Raeker, M. O., Borisov, A. B., Westfall, M. V. and Russell, M. W. (2007). Obscurin-like 1, OBSL1, is a novel cytoskeletal protein related to obscurin. *Genomics* **89**, 521-531.

Hackman, P., Vihola, A., Haravuori, H., Marchand, S., Sarparanta, J., De Seze, J., Labeit, S., Witt, C., Peltonen, L., Richard, I. et al. (2002). Tibial muscular dystrophy is a titinopathy caused by mutations in TTN, the gene encoding the giant skeletal-muscle protein titin. *Am. J. Hum. Genet.* **71**, 492-500.

Hsu, Y. J. and Goodman, S. R. (2005). Spectrin and ubiquitination: a review. *Cell Mol. Biol. (Noisy-le-grand) Suppl.* **51**, OL801-OL807.

Knollmann, B. C., Chopra, N., Hlaing, T., Akin, B., Yang, T., Ettensohn, K., Knollmann, B. E., Horton, K. D., Weissman, N. J., Holinstat, I. et al. (2006). Casq2 deletion causes sarcoplasmic reticulum volume increase, premature Ca2+ release, and catecholaminergic polymorphic ventricular tachycardia. *J. Clin. Invest.* **116**, 2510-2520.

Kontrogianni-Konstantopoulos, A., Jones, E. M., Van Rossum, D. B. and Bloch, R. J. (2003). Obscurin is a ligand for small ankyrin 1 in skeletal muscle. *Mol. Biol. Cell* **14**, 1138-1148.

Kontrogianni-Konstantopoulos, A., Catino, D. H., Strong, J. C., Sutter, S., Borisov, A. B., Pumplin, D. W., Russell, M. W. and Bloch, R. J. (2006). Obscurin modulates the assembly and organization of sarcomeres and the sarcoplasmic reticulum. *FASEB J.* **20**, 2102-2111.

Lange, S., Auerbach, D., McLoughlin, P., Perriard, E., Schafer, B. W., Perriard, J. C. and Ehler, E. (2002). Subcellular targeting of metabolic enzymes to titin in heart muscle may be mediated by DRAL/FHL-2. *J. Cell Sci.* **115**, 4925-4936.

Mendez, J. and Keys, A. (1960). Density and composition of mammalian muscle. *Metabolism* **9**, 184-188.

Mohler, P. J. (2006). Ankyrins and human disease: what the electrophysiologist should know. *J. Cardiovasc. Electrophysiol.* **17**, 1153-1159.

Mohler, P. J., Gramolini, A. O. and Bennett, V. (2002). The ankyrin-B C-terminal domain determines activity of ankyrin-B/G chimeras in rescue of abnormal inositol 1,4,5-trisphosphate and ryanodine receptor distribution in ankyrin-B (–/–) neonatal cardiomyocytes. *J. Biol. Chem.* **277**, 10599-10607.

Mohler, P. J., Yoon, W. and Bennett, V. (2004). Ankyrin-B targets beta2-spectrin to an intracellular compartment in neonatal cardiomyocytes. *J. Biol. Chem.* **279**, 40185-40193.

Mohler, P. J., Davis, J. Q. and Bennett, V. (2005). Ankyrin-B coordinates the Na/K ATPase, Na/Ca exchanger, and InsP3 receptor in a cardiac T-tubule/SR microdomain. *PLoS Biol.* **3**, e423.

Morii, H., Takisawa, H. and Yamamoto, T. (1985). Inactivation of a Ca^{2+}-induced Ca^{2+} release channel from skeletal muscle sarcoplasmic reticulum during active Ca^{2+} transport. *J. Biol. Chem.* **260**, 11536-11541.

Oved, S., Mosesson, Y., Zwang, Y., Santonico, E., Shtiegman, K., Marmor, M. D., Kochupurakkal, B. S., Katz, M., Lavi, S., Cesareni, G. et al. (2006). Conjugation to Nedd8 instigates ubiquitylation and down-regulation of activated receptor tyrosine kinases. *J. Biol. Chem.* **281**, 21640-21651.

Pan, Z. Q., Kentsis, A., Dias, D. C., Yamoah, K. and Wu, K. (2004). Nedd8 on cullin: building an expressway to protein destruction. *Oncogene* **23**, 1985-1997.

Pierobon-Bormioli, S., Angelini, C., Armani, M. and Testa, G. F. (1981). Myopathological findings in progressive myoclonus epilepsy. *Acta Neuropathol. Suppl.* **7**, 334-337.

Porter, N. C., Resneck, W. G., O'Neill, A., Van Rossum, D. B., Stone, M. R. and Bloch, R. J. (2005). Association of small ankyrin 1 with the sarcoplasmic reticulum. *Mol. Membr. Biol.* **22**, 421-432.

Qadota, H., McGaha, L. A., Mercer, K. B., Stark, T. J., Ferrara, T. M. and Benian, G. M. (2008). A novel protein phosphatase is a binding partner for the protein kinase domains of UNC-89 (Obscurin) in Caenorhabditis elegans. *Mol. Biol. Cell* **19**, 2424-2432.

Quarta, M., Giacomello, E., Toniolo, L., Cusimano, V., Birkenmeier, C., Peters, L., Sorrentino, V. and Reggiani, C. (2007). Abstracts of the IV IIM Meeting-Rome (Italy), November 21-24, 2007. *Basic Appl. Myol.* **17**, 251-267.

Raeker, M. O., Su, F., Geisler, S. B., Borisov, A. B., Kontrogianni-Konstantopoulos, A., Lyons, S. E. and Russell, M. W. (2006). Obscurin is required for the lateral alignment of striated myofibrils in zebrafish. *Dev. Dyn.* **235**, 2018-2029.

Rossi, A. E. and Dirksen, R. T. (2006). Sarcoplasmic reticulum: the dynamic calcium governor of muscle. *Muscle Nerve* **33**, 715-731.

Rossi, D., Barone, V., Giacomello, E., Cusimano, V. and Sorrentino, V. (2008). The sarcoplasmic reticulum: an organized patchwork of specialized domains. *Traffic* **9**, 1044-1049.

Sacks, R. D. and Roy, R. R. (1982). Architecture of the hind limb muscles of cats: functional significance. *J. Morphol.* **173**, 185-195.

Sam, M., Shah, S., Friden, J., Milner, D. J., Capetanaki, Y. and Lieber, R. L. (2000). Desmin knockout muscles generate lower stress and are less vulnerable to injury compared with wild-type muscles. *Am. J. Physiol. Cell Physiol.* **279**, C1116-C1122.

Small, T. M., Gernert, K. M., Flaherty, D. B., Mercer, K. B., Borodovsky, M. and Benian, G. M. (2004). Three new isoforms of Caenorhabditis elegans UNC-89 containing MLCK-like protein kinase domains. *J. Mol. Biol.* **342**, 91-108.

Tuvia, S., Buhusi, M., Davis, L., Reedy, M. and Bennett, V. (1999). Ankyrin-B is required for intracellular sorting of structurally diverse Ca2+ homeostasis proteins. *J. Cell Biol.* **147**, 995-1008.

Udd, B., Vihola, A., Sarparanta, J., Richard, I. and Hackman, P. (2005). Titinopathies and extension of the M-line mutation phenotype beyond distal myopathy and LGMD2J. *Neurology* **64**, 636-642.

Van den Bergh, P. Y., Bouquiaux, O., Verellen, C., Marchand, S., Richard, I., Hackman, P. and Udd, B. (2003). Tibial muscular dystrophy in a Belgian family. *Ann. Neurol.* **54**, 248-251.

Warren, C. M., Krzesinski, P. R. and Greaser, M. L. (2003). Vertical agarose gel electrophoresis and electroblotting of high-molecular-weight proteins. *Electrophoresis* **24**, 1695-1702.

Xirodimas, D. P., Saville, M. K., Bourdon, J. C., Hay, R. T. and Lane, D. P. (2004). Mdm2-mediated NEDD8 conjugation of p53 inhibits its transcriptional activity. *Cell* **118**, 83-97.

Young, P., Ehler, E. and Gautel, M. (2001). Obscurin, a giant sarcomeric Rho guanine nucleotide exchange factor protein involved in sarcomere assembly. *J. Cell Biol.* **154**, 123-136.

Zhang, Q., Skepper, J. N., Yang, F., Davies, J. D., Hegyi, L., Roberts, R. G., Weissberg, P. L., Ellis, J. A. and Shanahan, C. M. (2001). Nesprins: a novel family of spectrin-repeat-containing proteins that localize to the nuclear membrane in multiple tissues. *J. Cell Sci.* **114**, 4485-4498.

Zhou, Q., Chu, P. H., Huang, C., Cheng, C. F., Martone, M. E., Knoll, G., Shelton, G. D., Evans, S. and Chen, J. (2001). Ablation of Cypher, a PDZ-LIM domain Z-line protein, causes a severe form of congenital myopathy. *J. Cell Biol.* **155**, 605-612.